Mononuclear Four-Coordinate Bis-Fluoride Bis-NHC Complexes of Chromium(II), Iron(II), and Cobalt(II)

Carlos M. Acosta,[1] Dmitry S. Belov,[1] Andy H. Lamur,[1] ChristiAnna L. Brantley,[2] Xavier Solans-Monfort,[3] Kelly L. Rue,[1] George Christou,[2] and Konstantin V. Bukhryakov[1,]*

[1]Department of Chemistry and Biochemistry, Florida International University, Miami, FL 33199, USA

[2]Department of Chemistry, University of Florida, Gainesville, FL 32611, USA

[3]Departament de Química, Universitat Autònoma de Barcelona, 08193 Bellaterra, Spain

ABSTRACT

The reaction between silylamido complexes of Cr(II), Fe(II), and Co(II) and IMes•2HF salt in the presence of IMes (IMes = 1,3-dimesitylimidazol-2-ylidene) led to isolation of $Cr(IMes)_2(F)_2$ (**2-Cr**), $Fe(IMes)_2(F)_2$ (**2-Fe**), and $Co(IMes)_2(F)_2$ (**2-Co**). X-ray structural studies revealed that **2-Cr** adopts square planar geometry, while **2-Fe** and **2-Co** have distorted tetrahedral geometry. Magnetic susceptibility studies of **2-Cr**, **2-Fe**, and **2-Co** were consistent with high spin complexes, S = 2 for **2-Cr**/**2-Fe** and S = 3/2 for **2-Co**. We demonstrated that fluoride can be successfully exchanged for cyanide and azide using trimethylsilyl cyanide and trimethylsilyl azide (**3-Fe** and **4-Fe**). DFT studies suggest that **2-Cr** preference to adopt square planar geometry over tetrahedral is due to its d^4 metal center, where four electrons fill the lower-lying d-orbitals.

INTRODUCTION

Organometallic fluoride complexes present an attractive class of compounds that have found application in numerous catalytic transformations.[1, 2] Systems based on first-row transition metal fluorides are particularly interesting due to their abundance and low cost. Specific applications include olefin polymerization,[3] hydrosilylation,[4, 5] hydrodefluorination of fluoroolefins,[6, 7] C−F bond activation,[8] and fluorination of alkyl halides and triflates.[9] Among those systems, Fe-mediated transformations received special attention.[10] Organometallic Fe fluoride complexes are considered to be active species in cross-coupling reactions,[11-15] defluoroborylation of aryl fluorides,[16] C–F and C–H activation of fluoroarenes,[17, 18] and hydrodimerization of fluoroalkenes.[19]

Besides the versatile application of metal fluorides in catalysis, those complexes are utilized in synthesis, taking advantage of the high affinity between F and Si atoms. Thus, the reaction between L_nM−F and Me_3Si−R allows the substitution of fluorine by a wide variety of R groups under mild conditions.[20-23] The volatile byproduct, Me_3SiF, can be easily traced by ^{29}Si and ^{19}F NMR spectroscopy.

The common methods of synthesis of organometallic fluorides include late-stage fluorine atom incorporation utilizing salt metathesis in the presence of fluoride anion source (NaF, KF, NR_4F, TlF, or Cp_2CoF), abstraction of chloride with AgOTf or $AgBF_4$ followed by a source of fluoride (TAS-F, NR_4F), abstraction of Cl using AgF, the reaction of alkyl complexes with Me_3SnF, and protonation of alkyl, hydride, hydroxide, and alkoxide complexes by HF•base.[1, 7, 24-30] In contrast to organometallic chloride and bromide complexes that are often made from corresponding readily available inorganic halides, inorganic fluorides are not commonly used as starting materials. For instance, reactions between FeX_2 (X = Cl or Br) in the presence of N-heterocyclic carbenes

(NHCs) readily result in corresponding $Fe(NHC)_2X_2$ complexes.[31, 32] Similar reactions between FeF_2 and NHCs are not reported. Furthermore, our attempts to expose FeF_2 to various NHCs did not result in $Fe(NHC)_2F_2$ formation. This difference in reactivity can most likely be attributed to the greater stability of the metal fluoride's crystal structure, resulting from a small size of fluoride, which is evident when comparing lattice energies ($FeCl_2$ 2641 KJ/mol vs. FeF_2 2967 KJ/mol).[33] Herein, we present an early-stage incorporation of fluorine atoms into organometallic complexes utilizing the reaction between silylamido complexes of Cr(II), Fe(II), and Co(II) and IMes•2HF salt (IMes = 1,3-dimesitylimidazol-2-ylidene). We also report the synthetic utility of $Fe(IMes)_2F_2$ to introduce azide and cyanide ligands taking advantage of the strength of the Si−F bond.

IMes•2HF was obtained in the reaction between IMes and Et_3N•3HF in 90% yield. Four complexes, $Cr[N(SiMe_2Ph)_2]_2(THF)_2$ (**1-Cr**),[34] $Mn[N(SiMe_2Ph)_2]_2$ (**1-Mn**),[34] $Fe[N(SiMe_3)_2]_2$ (**1-Fe**),[35] and $Co[N(SiMe_2Ph)_2]_2(THF)$ (**1-Co**),[34] were subjected to 1 equiv. of IMes•2HF in the presence of 1 equiv. of free IMes in Et_2O yielding $Cr(IMes)_2(F)_2$ (**2-Cr**), $Fe(IMes)_2(F)_2$ (**2-Fe**), and $Co(IMes)_2(F)_2$ (**2-Co**), (Scheme 1).

Scheme 1. Synthesis of complexes **2**.

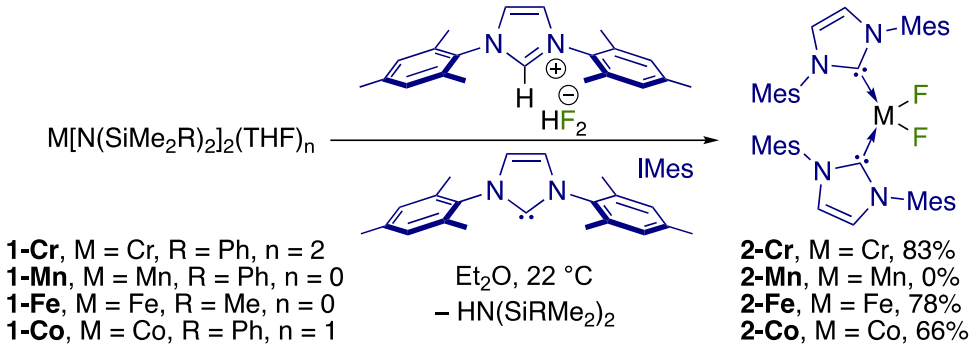

Complexes **2-Cr**, **2-Fe**, and **2-Co** were obtained in 83%, 78%, and 66% yields, respectively. All attempts to isolate **2-Mn** were unsuccessful, only protonated $HN(SiMe_2Ph)_2$ and free IMes were obtained in all cases, suggesting that a reaction occurred, but **2-Mn**, if formed, might have limited

stability. Thus, DFT calculations suggest that **2-Mn** is more prone to dissociate the IMes ligand than **2-Fe**, **2-Cr**, and **2-Co** (Figure S23). Reactions at lower temperatures did not lead to the isolation of **2-Mn**.

RESULTS AND DISCUSSION

All three isolated complexes, **2-Cr**, **2-Fe**, and **2-Co**, have a good solubility in dichloromethane, partial solubility in benzene, toluene, and THF, low solubility in Et_2O, and they are insoluble in pentane.

Structural Description. The X-ray structural studies revealed that **2-Cr**, **2-Fe**, and **2-Co** are mononuclear four-coordinate bis-fluoride bis-NHC complexes. Selected X-ray data for complexes **2-Cr**, **2-Fe**, and **2-Co** are shown in Table 1. **2-Cr** (Figure 1) adopted square planar geometry, and complexes **2-Fe** (Figure 2) and **2-Co** (Figure 3) have a distorted tetrahedral geometry. ^{1}H NMR spectra of **2-Cr**, **2-Fe**, and **2-Co** showed broad peaks in a range of 0 to +30 ppm, suggesting that those complexes are high-spin.

Table 1. Selected X-ray data for complexes **2-Cr**, **2-Fe**, and **2-Co**.

	M−F [Å]	M−C [Å]	F−M−F [°]	C−M−C [°]	F−M−C [°]
2-Cr	1.9124(10)	2.1752(17)	180.0	180.00(6)	89.89(6), 90.11(6)
2-Fe	1.872(3), 1.877(3)	2.146(4)	116.00(13)	118.74(16)	100.83(14), 106.16(14), 106.94(14), 108.61(14)
2-Co	1.880(4), 1.894(4)	2.077(6), 2.093(6)	107.15(17)	121.9(2)	102.15(19), 106.78(19), 108.43(19), 109.6(2)

Organometallic mononuclear Cr fluoride complexes are rare.[36] The Cr−F distance in **2-Cr** (1.9124(10) Å) is shorter compared to bond distances in reported square-planar fluoride bridged dimer, $[ArCr(\mu\text{-}F)(THF)]_2$ (1.970(2) Å and 2.104(2) Å), which appears to be the only other structurally characterized, organometallic Cr(II) fluoride.[37] Although $Cr(IMes)_2X_2$ (X = Cl or Br)

have not been reported, complexes of the type of $Cr(NHC)_2X_2$ (X = Cl[38, 39] or Br[40]) also adopt square-planar geometry.

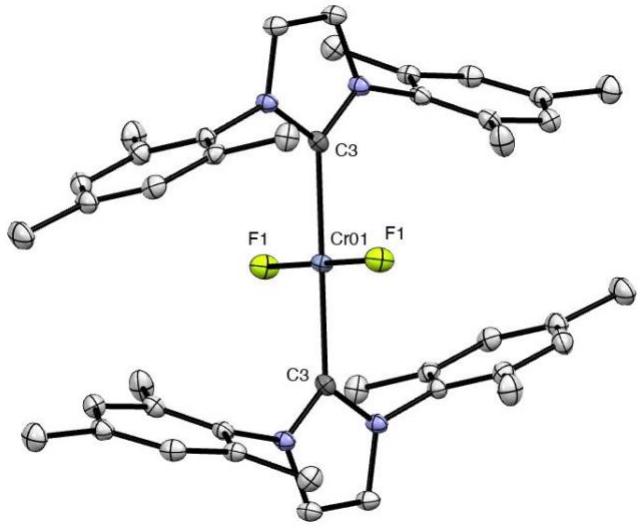

Figure 1. Perspective view of the crystal structure of complex **2-Cr** with thermal ellipsoids shown at 30% probability.

The number of crystallographically characterized organometallic Fe fluoride complexes is limited.[7, 23, 41, 42] To the best of our knowledge, the only reported mononuclear four-coordinate organometallic Fe fluoride complex contains tridentate tris(carbene)borate ligand.[23] The reported complex has a slightly shorter Fe−F distance (1.848 Å) compared to those in **2-Fe** (1.872(3) Å and 1.877(3) Å). Fe−C bond length in **2-Fe** (2.146(4) Å) is similar to those in $Fe(IMes)_2Cl_2$ (2.139(3) Å and 2.157(3) Å).[32] The C−Fe−C angle in **2-Fe** (118.74(16)°) is smaller than in $Fe(IMes)_2Cl_2$ (125.2(1)°) and the X−Fe−X angle is larger for a fluoride complex (116.00(13)° vs. 106.66(4)°, X = F vs. Cl, respectively). Since Fe−F bonds (1.872(3) Å and 1.877(3) Å) are significantly shorter than Fe−Cl bonds (2.292(1) Å and 2.310(1) Å), and fluorine, being the most electronegative element, has a highly localized electron density; we propose that the larger F−Fe−F angle is due higher electrostatic repulsion between two fluorine atoms in **2-Fe**, that are significantly closer to

the metal center, compared to the repulsion of two chloride atoms in $Fe(IMes)_2Cl_2$ that are further away. As a result, the C−Fe−C angle becomes smaller in **2-Fe.**

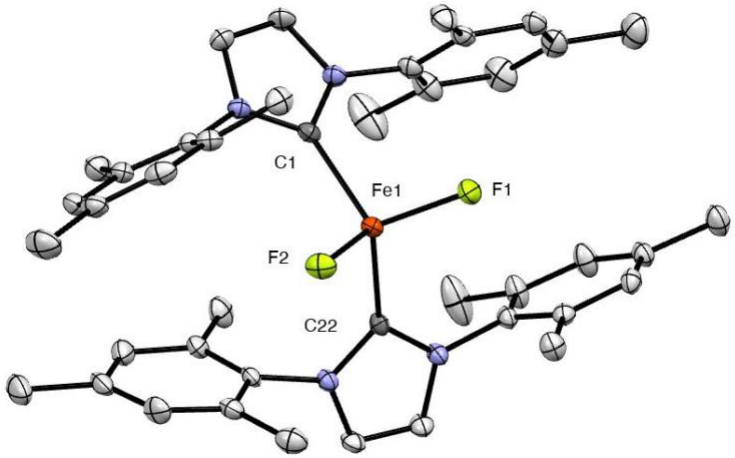

Figure 2. Perspective view of the crystal structure of complex **2-Fe** with thermal ellipsoids shown at 30% probability.

Several organometallic fluoride complexes of Co(III) are known.[43-46] Two crystallographically characterized organometallic Co(II) complexes are three-[47] and five-coordinate.[8] Therefore, no direct comparison between reported complexes and **2-Co** can be made. Co−C bond distances in **2-Co** (2.077(6) Å and 2.093(6) Å) are similar to those in $Co(IMes)_2Cl_2$ (2.069(2) Å and 2.089(2) Å)[48] and in $Co(IMes)_2Br_2$ (2.082(3) Å).[49] The C−Co−C angle in **2-Co** (121.9(2)°) is slightly smaller than those in $Co(IMes)_2Cl_2$ (124.95(9)°) and $Co(IMes)_2Br_2$ (130.4(1)°) and the X−Co−X angle is slightly larger (107.15(17)°, 103.21(3)°, and 103.9(1)°, in the row X = F, Cl, and Br, respectively). Similarly, to **2-Fe**, we explain a larger F−Co−F angle by electrostatic repulsion of two fluorine atoms in **2-Co**.

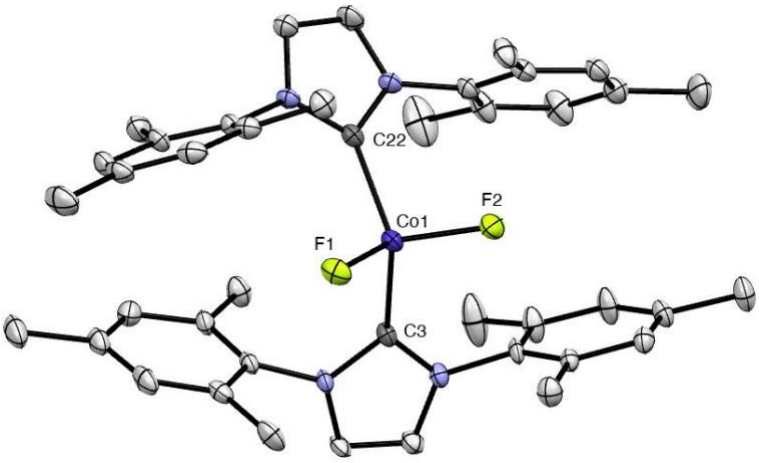

Figure 3. Perspective view of the crystal structure of complex **2-Co** with thermal ellipsoids shown at 30% probability.

The bis-fluoride bis-NHC Fe(II) complex, **2-Fe,** readily reacts with $TMSN_3$ and TMSCN to provide corresponding bis-azide and bis-cyanide complexes **3-Fe** and **4-Fe** in 42% and 67% yields, respectively (Scheme 2).

Scheme 2. Synthesis of complexes 3-Fe and 4-Fe.

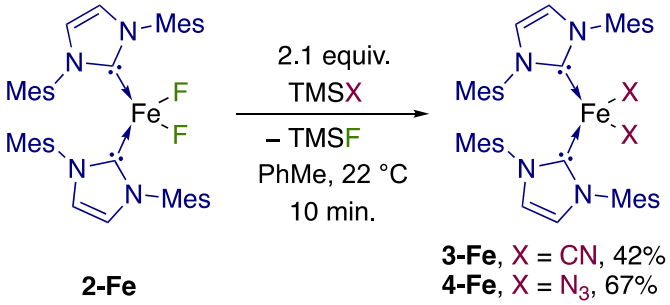

Unfortunately, multiple attempts to obtain the crystal structure of **3-Fe** were unsuccessful. This compound has a strong tendency to grow in stacks of thin sheets which are unaligned (Figures S4-6). Attempts to isolate a single layer resulted in a thin sheet that scattered poorly and yielded no meaningful structural data. Despite this, elemental analysis of **3-Fe** does support the proposed structure. In addition, ^1H NMR showed relatively sharp peaks in a range of – 3.5 to +4.5 ppm (CD_2Cl_2), which can be assigned, suggesting an intermediate spin state for Fe, which is expected

for strong field ligands, such as cyanide. The IR spectrum of **3-Fe** shows one cyanide stretch at 2102 cm^{-1}, corresponding to a square planar complex with two cyanides in the trans position. DFT results further support a square planar geometry (Figure S22). Noteworthy, reported $Fe(IMes)_2(Me)_2$, containing strong field ligand, also adopts a square planar geometry.[50]

In contrast to **3-Fe**, complex **4-Fe** gave crystals suitable for X-ray structural studies (Figure 4). Crystallographic studies show **4-Fe** adopts a distorted tetrahedral geometry [N–Fe–N 110.46(8) °, C–Fe–C 128.27(9) °].

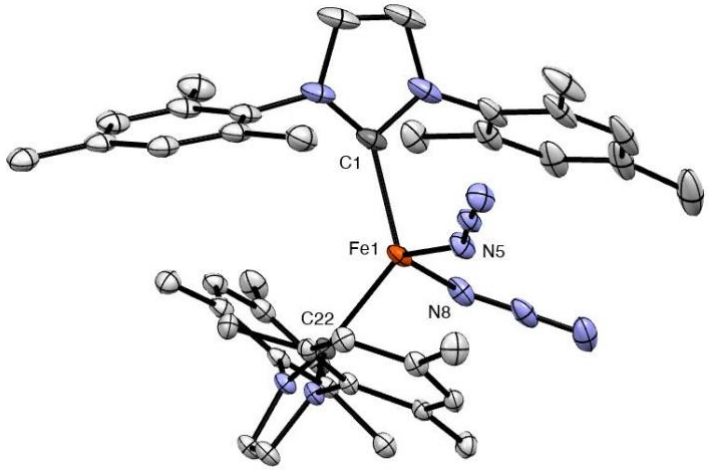

Figure 4. Perspective view of the crystal structure of complex **4-Fe** with thermal ellipsoids shown at 30% probability.

Crystallographically characterized mononuclear four-coordinate organometallic Fe azides contain bidentate[51] or tridentate[52-56] ligands and only one azide attached to Fe with a Fe–N bond distances in a range of 1.91–2.06 Å. Fe−N bond lengths in **4-Fe** are in the same range (1.9826(16) Å and 1.9913(19) Å). Fe−C bond lengths in **4-Fe** (2.1238(17) Å and 2.155(2) Å) are similar to those in **2-Fe**.

We found that **4-Fe** has limited stability, especially when exposed to light. Photolysis of Fe(II) complexes containing one azide ligand has been extensively utilized to prepare Fe(IV) terminal

nitrides.[52, 53, 57, 58] Photolysis of **4-Fe** at 395 nm led to an unidentified mixture of decomposition products. Due to the limited stability of **4-Fe**, all attempts to obtain a pure sample, confirmed by elemental analysis, were unsuccessful. Therefore, we were unable to perform magnetic measurements of complex **4-Fe**.

Magnetic susceptibility studies. Variable-temperature dc magnetic susceptibility (χ_M) data were collected on crushed, vacuum-dried microcrystalline samples in the 5.0 – 300 K range in a 0.10 T (1.0 kG) applied dc field and plotted as $\chi_M T$ vs T (Figure 5). For **2-Cr**, $\chi_M T$ is 2.61 cm^3 K mol^{-1} at 300 K and remains essentially constant with decreasing temperture until a small decrease below ~15 K to reach 2.26 cm^3 K mol^{-1} at 5.0 K (Figure 5A). The data confirm the square planar Cr^{II} ion to be high-spin with spin $S = 2$ and $g < 2$ slightly, as expected for a less than half-filled shell; the spin-only ($g = 2.0$) $\chi_M T$ is 3.0 cm^3 K mol^{-1}. The ac in-phase $\chi'_M T$ vs T plot (Figure S8, SI) agrees with the dc plot and supports the conclusion of a high-spin $S = 2$ Cr^{II}.

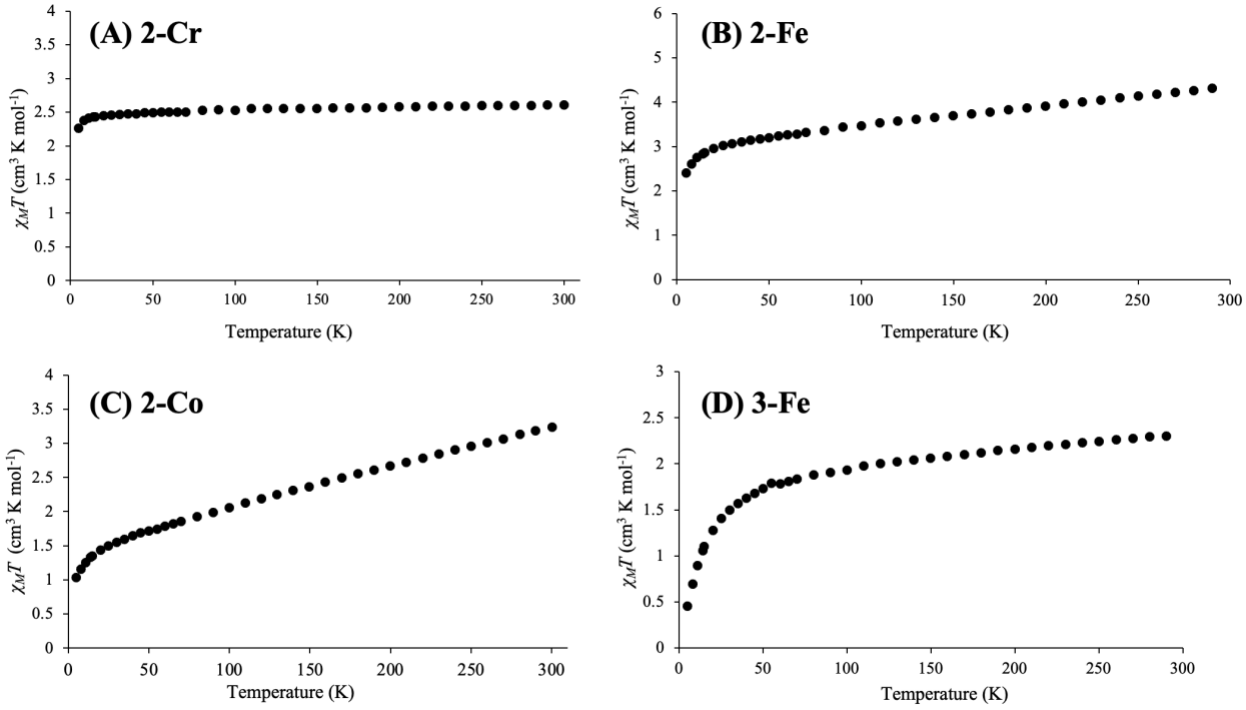

Figure 5. SQUID measurements $\chi_M T$ vs T plots of (A) **2-Cr**, (B) **2-Fe**, (C) **2-Co**, and (D) **3-Fe**.

For **2-Fe**, the complex contains an Fe^{II} ion in distorted-tetrahedral geometry and is thus expected to be high-spin $S = 2$ similar to a previously published complex, $Fe(IMes)_2(Cl)_2$.[59] $\chi_M T$ at 300 K is 4.35 cm^3 K mol^{-1}, which is significantly higher than the spin-only ($g = 2.0$) value of 3.0 cm^3 K mol^{-1} for $S = 2$, steadily decreases with decreasing T to 2.96 cm^3 K mol^{-1} at 20.0 K, and then dips to a final 2.39 cm^3 K mol^{-1} at 5.0 K (Figure 5B). The ac in-phase $\chi'_M T$ vs T plot (Figure S10) agrees with the low-T dc data and supports the conclusion of a high-spin $S = 2$ Fe^{II}. For **2-Co**, the complex contains a Co^{II} ion in distorted-tetrahedral geometry and is expected to be high-spin $S = {}^3/_2$. $\chi_M T$ is 3.23 cm^3 K mol^{-1} at 300 K, which is much higher than the spin-only $S = {}^3/_2$ value of 1.88 cm^3 K mol^{-1}, and then steadily decreases to 1.43 cm^3 K mol^{-1} at 20.0 K and then dips to a final 1.03 cm^3 K mol^{-1} at 5.0 K (Figure 5C). The ac in-phase $\chi'_M T$ vs T plot (Figure S12) agrees with the low-T dc data and supports the conclusion of a high-spin $S = {}^3/_2$ Co^{II} similar to $Co(IMes)_2(Cl)_2$.[60] For both **2-Fe** and **2-Co**, the $\chi_M T$ at higher temperatures being significantly larger than the spin-only value is assigned to significant intrinsic magnetic anisotropy and resulting $g > 2$ for these ions from orbital angular momentum, as seen also in other distorted tetrahedral systems.[61]

For **3-Fe**, the $\chi_M T$ at 300 K is 2.30 cm^3 K mol^{-1}, decreasing to 0.45 cm^3 K mol^{-1} at 5.0 K (Figure 5D). The 5.0 K value and the plot profile suggest an $S = 0$ ground state consistent with square planar geometry and the strong-field CN^- ligands. This is supported by the low-temperature ac susceptibility, the $\chi'_M T$ decreasing from 1.13 cm^3 K mol^{-1} at 15 K to 0.18 cm^3 K mol^{-1} at 1.8 K and clearly heading for 0 (Figure S17). The increasing $\chi_M T$ with increasing T is consistent with population of $S = 1$ excited states with significant magnetic anisotropy. Another possibility consistent with the lowest-T data is that 3-Fe has an $S = 1$ ground state and the decrease below

~100 K is due to intermolecular antiferromagnetic interactions, but the feasibility of this cannot be assessed without the crystal structure.

Variable-frequency ac out-of-phase (χ''_M) susceptibility studies were carried out on **2-Cr**, **2-Fe,** and **2-Co** in the 1.8 – 15 K range using a 3.5 G ac field and oscillation frequencies of 50, 250, and 997 Hz. None of the complexes exhibited χ''_M signals down to 1.8 K. Additional ac studies in the presence of an applied dc field (0.1 T) were carried out to probe whether one or more of the compounds might exhibit field-induced single-molecule magnet (SMM) behavior. Indeed, in the applied dc field compound **2-Co** revealed clear frequency-dependent out-of-phase χ''_M signals in the 1.8 – 4 K range and a concomitant decrease in the in-phase $\chi'_M T$. The χ''_M vs T data were used to construct an Arrhenius plot of $\ln(1/\tau)$ vs $1/T_{max}$, where τ is the relaxation time, giving an effective barrier to magnetization relaxation of U_{eff} = 27.1 K and $1/\tau_o = 5.6 \times 10^8\ s^{-1}$, typical values for four-coordinate Co SMM compounds range from 6.3 K to 118 K, with the mean value being 37.0 K (Figure S16). Many four-coordinate Co^{II} compound have a U_{eff} between 20 – 30 K.[62] Compounds **2-Fe**, **3-Fe**, and **2-Cr** did not exhibit χ''_M signals in the presence of a dc field.

It is interesting to note that the main difference between **2-Fe** and **3-Fe** is a change in the ligand field. **2-Fe** and **3-Fe** both contain a four-coordinate Fe^{II} with two bound IMes ligands; however, **2-Fe** has two F^- ligands while **3-Fe** has two CN^-. Fluoride is a weak field ligand, while cyanide is a strong field ligand. Having fluorine bound to the metal center decreases the splitting of the d orbitals, thus $\Delta_t <$ pairing energy, resulting in a high spin configuration of the d-electrons. For **3-Fe**, the reverse is true, $\Delta_t >$ pairing energy, resulting in a low-spin complex. This is nicely reflected in the magnetic measurements.

DFT Calculations. DFT (OPBE-D3)[63-65] calculations (see the computational details section for further information) on the three synthetized $MF_2(IMes)_2$ complexes predict that the most stable

coordination around the metal center is square planar for Cr and tetrahedral for Fe and Co (Figure S19) in agreement with X-ray diffraction structures. The resulting geometry is close to the X-ray structure, the largest variations being on Fe−C bond distances and C−Fe−C bond angles which are about 0.04 Å and 10 degrees, respectively. The tetrahedral coordination around Cr is unstable and all our attempts to find a local minimum evolved to the square planar structure. Moreover, the optimized structure imposing F−Cr−F and IMes−Cr−IMes angles close to the X-ray structure of **2-Co** is 18.0 kcal mol^{-1} higher in Gibbs energy than the square planar structure. For **2-Fe** and **2-Co** both the square planar and the tetrahedral coordination around metal center are minima of the potential energy surface but the latter is lower in Gibbs energy by 1.7 and 10.2 kcal mol^{-1}, respectively.

Analysis of the molecular orbitals (Figure 6) allows rationalizing the different structure for **2-Cr** with respect to **2-Fe** and **2-Co**. The d orbital splitting (Figure 6a) of an ideal square planar ligand field is characterized by four low-lying d orbitals and the d_{x2-y2} lying significantly above the other four. The ligand field of an ideal tetrahedral complex has two low lying degenerate orbitals and three slightly higher in energy orbitals. The nature of the occupied metal d orbitals and the energies of the associated molecular orbitals of **2-Cr**, **2-Fe** and **2-Co** for both the square planar and tetrahedral structures reasonably agree with this idealized picture, despite deviations from the ideal structure and the presence of p-bonding with F and NHC ligands (Figure 6b). The low-lying orbitals of the square planar coordination tend to be lower in energy than the five d orbitals of the tetrahedral environment, but the d_{x2-y2} orbital is much higher in energy. Accordingly, **2-Cr**, which formally has a d^4 metal center, prefers to be square planar and singly occupy the four low-lying orbitals of this structure. In contrast **2-Fe** and **2-Co** with a formal d^6 and a d^7 metal center prefer to have a tetrahedral coordination that avoids occupying the highly energetic d_{x2-y2} molecular

orbital of the square planar structure. Remarkably, calculations for **2-Fe** and **2-Co** suggest that an intermediate spin square planar structure where the d_{x2-y2} orbital is not occupied is similar in energy to the high spin square planar structure but it is always less stable than the tetrahedral one.

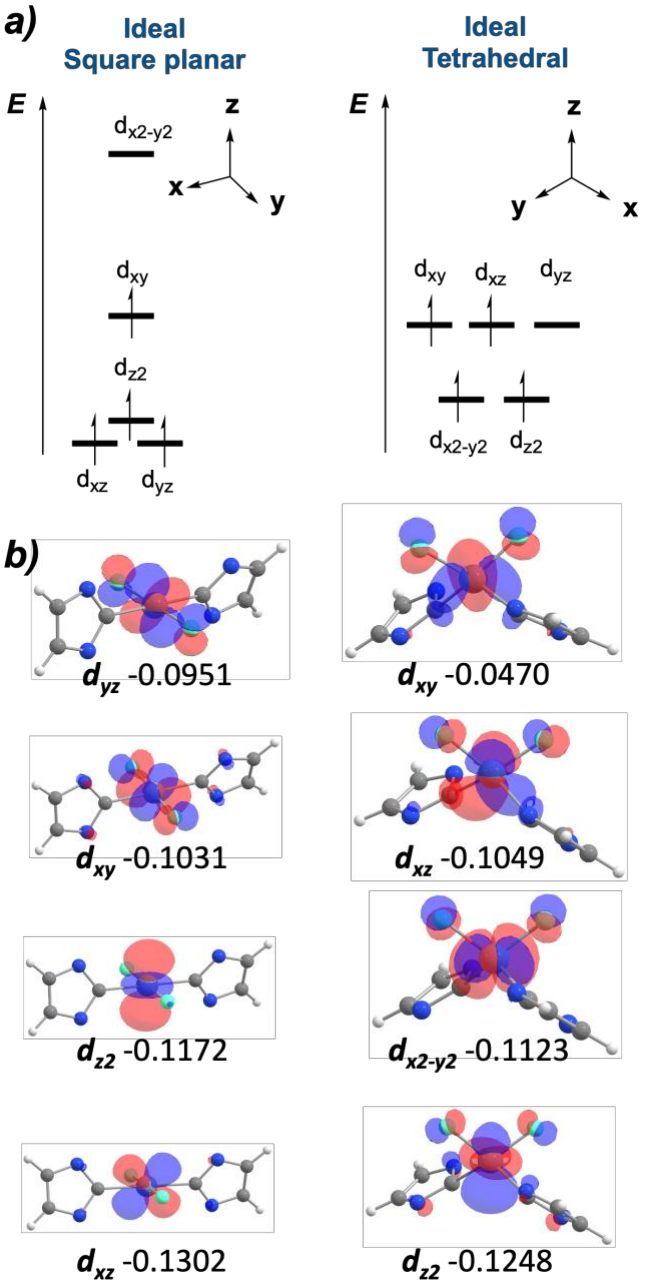

Figure 6. (a) Ligand field for an ideal square planar and tetrahedral complex. (b) Singly occupied molecular orbitals for **2-Cr** with square planar and tetrahedral coordination around the metal center.

CONCLUSION

We have outlined a new synthetic route into the first-row organometallic fluoride complexes utilizing metal silylamido complexes and IMes•2HF salt. Using this method, three new complexes of the form $M(F)_2(IMes)_2$ were isolated (**2-Cr**, **2-Fe**, **2-Co**). Both **2-Fe** and **2-Co** adopt a distorted tetrahedral geometry, while **2-Cr** is square planar. Interestingly **2-Fe** and **2-Co** have larger X−M−X bond angles than the analogous chloride or bromide complexes ($M(X)_2(IMes)_2$, X = Cl, Br). We attribute this to the higher electron density on fluorine and the shorter M−X bond lengths leading to greater electrostatic repulsion between fluorine atoms compared to chlorine. The synthetic utility of **2-Fe** was also demonstrated by using TMSCN and $TMSN_3$ to substitute fluoride for cyanide and azide and yield **3-Fe** and **4-Fe**, respectively. Magnetic susceptibility studies for **2-Cr**, **2-Fe**, **2-Co** are consistent with high-spin Cr^{2+}/ Fe^{2+}/ Co^{2+}complexes with $S = 2$ for **2-Cr**/**2-Fe** and $S = 3/2$ for **2-Co**. **2-Co** was found to exhibit field-induced single-molecule magnet (SMM) behavior between 1.8 – 4 K, values for U_{eff} and $1/\tau_o$ were calculated and found to be consistent with four coordinate Co^{II} compounds (U_{eff} = 27.1 K, $1/\tau_o$ = 5.6 X 10^8 s^{-1}). As expected, the substitution of fluorides in **2-Fe** to strong field ligands (cyanides in **3-Fe**) led to a low spin Fe complex confirmed by magnetic measurements. DFT (OPBE-D3) calculations are consistent with experimental structural and magnetic studies. These calculations also offered insight on why **2-Cr** adopts square planar geometry rather than the tetrahedral geometry of **2-Fe** and **2-Co**.

ASSOCIATED CONTENT

The Supporting Information is available free of charge at

Synthesis details, NMR spectra, details of X-ray studies, and computational details (PDF)

Cartesian coordinates of the DFT structures (XYZ)

CCDC 2282175-2282178 contain the supplementary crystallographic data for this paper. These data can be obtained free of charge via www.ccdc.cam.ac.uk/data_request/cif, or by emailing data_request@ccdc.cam.ac.uk, or by contacting The Cambridge Crystallographic Data Centre, 12 Union Road, Cambridge CB2 1EZ, UK; fax: +44 1223 336033.

AUTHOR INFORMATION

Corresponding Author

Konstantin V. Bukhryakov − Department of Chemistry and Biochemistry, Florida International University, Miami, FL 33199, USA; orcid.org/0000-0002-8425-9671; Email: **kbukhrya@fiu.edu**

Authors

Carlos M. Acosta − Department of Chemistry and Biochemistry, Florida International University, Miami, FL 33199, USA

Dmitry S. Belov – Department of Chemistry and Biochemistry, Florida International University, Miami, FL 33199, USA

Andy H. Lamur − Department of Chemistry and Biochemistry, Florida International University, Miami, FL 33199, USA

ChristiAnna Brantley − Department of Chemistry, University of Florida, Gainesville, Florida 32611-7200, United States; orcid.org/0000-0003-3726-2904

Xavier Solans-Monfort − Departament de Química, Universitat Autònoma de Barcelona, 08193 Bellaterra, Spain; orcid.org/0000-0002-2172-3895

Kelly L. Rue – Department of Chemistry and Biochemistry, Florida International University, Miami, FL 33199, USA.

George Christou − Department of Chemistry, University of Florida, Gainesville, Florida 32611-7200, United States; orcid.org/0000-0001-5923-5523

Author Contributions

C.M.A, D.S.B, and A.H.L. performed the experiments and interpreted the results. C.B. and G.C. performed and interpreted magnetic measurements. X.S.-M. performed and interpreted DFT studies. K.L.R performed and interpreted X-ray studies. K.V.B. conceived the idea and supervised the whole work. C.M.A, C.B., G.C., X.S.-M., and K.V.B. have participated in the writing of the manuscript.

ACKNOWLEDGMENT

This work was supported by NSF grant CHE-2212944. The work at the University of Florida was supported by NSF Grant CHE-1900321. The work at the Universitat Autònoma de Barcelona was supported by the Spanish MICINN through the PID2020-112715GB-I00 project. K.L.R. was supported by the U.S. Nuclear Regulatory Commission (NRC) fellowship grant No. 31310018M0012 awarded to FIU. We are grateful to Indranil Chakraborty (FIU) and Khalil Abboud (UF) for X-ray studies.

REFERENCES

1. Murphy, E. F.; Murugavel, R.; Roesky, H. W., Organometallic Fluorides: Compounds Containing Carbon−Metal−Fluorine Fragments of d-Block Metals. *Chem. Rev.* **1997,** *97* (8), 3425-3468.

2. Nikiforov, G. B.; Roesky, H. W.; Koley, D., A survey of titanium fluoride complexes, their preparation, reactivity, and applications. *Coord. Chem. Rev.* **2014,** *258-259*, 16-57.

3. Wright, L. A.; Hope, E. G.; Solan, G. A.; Cross, W. B.; Singh, K., Active O,Npy,N-Titanium(IV) Fluoride Precatalysts for Ethylene Polymerization: Exploring "Fluoride Effects" on Polymer Properties and Catalytic Performance. *Organometallics* **2016,** *35* (9), 1183-1191.

4. Verdaguer, X.; Lange, U. E. W.; Reding, M. T.; Buchwald, S. L., Highly Enantioselective Imine Hydrosilylation Using (S,S)-Ethylenebis(η5-tetrahydroindenyl)titanium Difluoride. *J. Am. Chem. Soc* **1996,** *118* (28), 6784-6785.

5. Bareille, L.; Becht, S.; Cui, J. L.; Le Gendre, P.; Moïse, C., First Titanium-Catalyzed anti-1,4-Hydrosilylation of Dienes. *Organometallics* **2005,** *24* (24), 5802-5806.

6. Kuehnel, M. F.; Holstein, P.; Kliche, M.; Krüger, J.; Matthies, S.; Nitsch, D.; Schutt, J.; Sparenberg, M.; Lentz, D., Titanium-Catalyzed Vinylic and Allylic C−F Bond Activation—Scope, Limitations and Mechanistic Insight. *Chem. Eur. J* **2012,** *18* (34), 10701-10714.

7. Vela, J.; Smith, J. M.; Yu, Y.; Ketterer, N. A.; Flaschenriem, C. J.; Lachicotte, R. J.; Holland, P. L., Synthesis and Reactivity of Low-Coordinate Iron(II) Fluoride Complexes and Their Use in the Catalytic Hydrodefluorination of Fluorocarbons. *J. Am. Chem. Soc* **2005,** *127* (21), 7857-7870.

8. Lu, F.; Sun, H.; Li, X., Cobalt-catalyzed Selective C-F Bond Activation and Alkylation of Polyfluoroaryl Imines. *Chin. J. Chem* . **2013,** *31* (7), 927-932.

9. Lin, X.; Weng, Z., Transition metal complex assisted Csp3–F bond formation. *Dalton Trans.* **2015,** *44* (5), 2021-2037.

10. Rana, S.; Biswas, J. P.; Paul, S.; Paik, A.; Maiti, D., Organic synthesis with the most abundant transition metal–iron: from rust to multitasking catalysts. *Chem. Soc. Rev.* **2021,** *50* (1), 243-472.

11. Hatakeyama, T.; Nakamura, M., Iron-Catalyzed Selective Biaryl Coupling: Remarkable Suppression of Homocoupling by the Fluoride Anion. *J. Am. Chem. Soc* **2007,** *129* (32), 9844-9845.

12. Hatakeyama, T.; Hashimoto, S.; Ishizuka, K.; Nakamura, M., Highly Selective Biaryl Cross-Coupling Reactions between Aryl Halides and Aryl Grignard Reagents: A New Catalyst Combination of N-Heterocyclic Carbenes and Iron, Cobalt, and Nickel Fluorides. *J. Am. Chem. Soc* **2009,** *131* (33), 11949-11963.

13. Agata, R.; Takaya, H.; Matsuda, H.; Nakatani, N.; Takeuchi, K.; Iwamoto, T.; Hatakeyama, T.; Nakamura, M., Iron-Catalyzed Cross Coupling of Aryl Chlorides with Alkyl Grignard Reagents: Synthetic Scope and FeII/FeIV Mechanism Supported by X-ray Absorption Spectroscopy and Density Functional Theory Calculations. *Bull. Chem. Soc. Jpn.* **2018,** *92* (2), 381-390.

14. Mo, Z.; Zhang, Q.; Deng, L., Dinuclear Iron Complex-Catalyzed Cross-Coupling of Primary Alkyl Fluorides with Aryl Grignard Reagents. *Organometallics* **2012,** *31* (18), 6518-6521.

15. Luo, S.; Yu, D.-G.; Zhu, R.-Y.; Wang, X.; Wang, L.; Shi, Z.-J., Fe-promoted cross coupling of homobenzylic methyl ethers with Grignard reagents via sp3 C–O bond cleavage. *Chem. Commun.* **2013,** *49* (71), 7794-7796.

16. Zhao, X.; Wu, M.; Liu, Y.; Cao, S., LiHMDS-Promoted Palladium or Iron-Catalyzed ipso-Defluoroborylation of Aryl Fluorides. *Org. Lett.* **2018,** *20* (18), 5564-5568.

17. Zheng, T.; Li, J.; Zhang, S.; Xue, B.; Sun, H.; Li, X.; Fuhr, O.; Fenske, D., Selective C–F and C–H Activation of Fluoroarenes by Fe(PMe3)4 and Catalytic Performance of Iron Hydride in Hydrosilylation of Carbonyl Compounds. *Organometallics* **2016,** *35* (20), 3538-3545.

18. Wang, L.; Sun, H.; Li, X., Synthesis of Iron Hydrides by Selective C–F/C–H Bond Activation in Fluoroarylimines and Their Applications in Catalytic Reduction Reactions. *Eur. J. Inorg. Chem.* **2015,** *2015* (16), 2732-2743.

19. Ghostine, K.; Gabidullin, B. M.; Tom Baker, R., Synthesis and reactivity of perfluoroferracyclocarbenes. *Polyhedron* **2020,** *185*, 114587.

20. Vicente, J.; Gil-Rubio, J.; Guerrero-Leal, J.; Bautista, D., Synthesis of the First Family of Rhodium(I) Perfluoroalkyl Complexes from Rhodium(I) Fluoro Complexes. *Organometallics* **2004,** *23* (21), 4871-4881.

21. Braun, T.; Izundu, J.; Steffen, A.; Neumann, B.; Stammler, H.-G., Reactivity of a palladium fluoro complex towards silanes and Bu3SnCHCH2: catalytic derivatisation of pentafluoropyridine based on carbon–fluorine bond activation reactions. *Dalton Trans.* **2006,** (43), 5118-5123.

22. Erickson, K. A.; Lichtscheidl, A. G.; Monreal, M. J.; Nelson, A. T.; Scott, B. L.; Morris, D. E.; Kiplinger, J. L., Exploiting the reactivity of actinide fluoride bonds for the synthesis and characterization of a new class of monometallic bis(azide) uranium complexes. *J. Organomet. Chem.* **2018,** *857*, 180-186.

23. Valdez-Moreira, J. A.; Thorarinsdottir, A. E.; DeGayner, J. A.; Lutz, S. A.; Chen, C.-H.; Losovyj, Y.; Pink, M.; Harris, T. D.; Smith, J. M., Strong π-Backbonding Enables Record Magnetic Exchange Coupling Through Cyanide. *J. Am. Chem. Soc* **2019,** *141* (43), 17092-17097.

24. Doherty, N. M.; Hoffmann, N. W., Transition-metal fluoro compounds containing carbonyl, phosphine, arsine, and stibine ligands. *Chem. Rev.* **1991,** *91* (4), 553-573.

25. Bennett, B. K.; Harrison, R. G.; Richmond, T. G., Cobaltocenium Fluoride: A Novel Source of "Naked" Fluoride Formed by Carbon-Fluorine Bond Activation in a Saturated Perfluorocarbon. *J. Am. Chem. Soc* **1994,** *116* (24), 11165-11166.

26. Barthazy, P.; Togni, A.; Mezzetti, A., Catalytic Fluorination by Halide Exchange with 16-Electron Ruthenium(II) Complexes. X-ray Structure of [Tl(μ-F)2Ru(dppe)2]PF6. *Organometallics* **2001,** *20* (16), 3472-3477.

27. Grushin, V. V.; Marshall, W. J., Is Fluoride Bonded to Two Pd Acceptors Still Basic? Three CH2Cl2 Molecules Encapsulating a Pd2(μ-F)2 Square and New Implications for Catalysis. *Angew. Chem. Int. Ed.* **2002,** *41* (23), 4476-4479.

28. Herron, J. R.; Ball, Z. T., Synthesis and Reactivity of Functionalized Arylcopper Compounds by Transmetalation of Organosilanes. *J. Am. Chem. Soc* **2008,** *130* (49), 16486-16487.

29. Ding, K.; Dugan, T. R.; Brennessel, W. W.; Bill, E.; Holland, P. L., Synthesis, Properties, and Reactivity of Diketiminate-Supported Cobalt Fluoride Complexes. *Organometallics* **2009,** *28* (23), 6650-6656.

30. Levason, W.; Monzittu, F. M.; Reid, G., Coordination chemistry and applications of medium/high oxidation state metal and non-metal fluoride and oxide-fluoride complexes with neutral donor ligands. *Coord. Chem. Rev.* **2019,** *391*, 90-130.

31. Louie, J.; Grubbs, R. H., Highly active iron imidazolylidene catalysts for atom transfer radical polymerization. *Chem. Commun.* **2000,** (16), 1479-1480.

32. Przyojski, J. A.; Arman, H. D.; Tonzetich, Z. J., Complexes of Iron(II) and Iron(III) Containing Aryl-Substituted N-Heterocyclic Carbene Ligands. *Organometallics* **2012,** *31* (8), 3264-3271.

33. Jenkins, H. D. B.; Roobottom, H. K., Lattice Energies. In *CRC handbook of chemistry and physics*, 97th ed.; CRC Press: 2016; pp 12-22.

34. König, S. N.; Schädle, C.; Maichle-Mössmer, C.; Anwander, R., Silylamide Complexes of Chromium(II), Manganese(II), and Cobalt(II) Bearing the Ligands N(SiHMe2)2 and N(SiPhMe2)2. *Inorg. Chem.* **2014,** *53* (9), 4585-4597.

35. Broere, D. L. J.; Čorić, I.; Brosnahan, A.; Holland, P. L., Quantitation of the THF Content in Fe[N(SiMe3)2]2·xTHF. *Inorg. Chem.* **2017,** *56* (6), 3140-3143.

36. Harvey, B. G.; Arif, A. M.; Glöckner, A.; Ernst, R. D., SF6 as a Selective and Reactive Fluorinating Agent for Low-Valent Transition Metal Complexes. *Organometallics* **2007,** *26* (11), 2872-2879.

37. Wolf, R.; Ni, C.; Nguyen, T.; Brynda, M.; Long, G. J.; Sutton, A. D.; Fischer, R. C.; Fettinger, J. C.; Hellman, M.; Pu, L.; Power, P. P., Substituent Effects in Formally Quintuple-Bonded ArCrCrAr Compounds (Ar = Terphenyl) and Related Species. *Inorg. Chem.* **2007,** *46* (26), 11277-11290.

38. Jones, C.; Dange, D.; Stasch, A., Synthesis and Crystal Structures of Two N-Heterocyclic Carbene Adducts of CrCl2. *J. Chem. Crystallogr.* **2012,** *42* (5), 494-497.

39. Ai, P.; Danopoulos, A. A.; Braunstein, P., N-Phosphanyl- and N,N′-Diphosphanyl-Substituted N-Heterocyclic Carbene Chromium Complexes: Synthesis, Structures, and Catalytic Ethylene Oligomerization. *Organometallics* **2015,** *34* (16), 4109-4116.

40. Downing, S. P.; Guadaño, S. C.; Pugh, D.; Danopoulos, A. A.; Bellabarba, R. M.; Hanton, M.; Smith, D.; Tooze, R. P., Indenyl- and Fluorenyl-Functionalized N-Heterocyclic Carbene Complexes of Titanium, Zirconium, Vanadium, Chromium, and Yttrium. *Organometallics* **2007,** *26* (15), 3762-3770.

41. Butschke, B.; Fillman, K. L.; Bendikov, T.; Shimon, L. J. W.; Diskin-Posner, Y.; Leitus, G.; Gorelsky, S. I.; Neidig, M. L.; Milstein, D., How Innocent are Potentially Redox Non-Innocent Ligands? Electronic Structure and Metal Oxidation States in Iron-PNN Complexes as a Representative Case Study. *Inorg. Chem.* **2015,** *54* (10), 4909-4926.

42. Song, L.-C.; Gao, X.-Y.; Liu, W.-B.; Zhang, H.-T.; Cao, M., Synthesis, Characterization, and Reactions of Functionalized Nickel–Iron Dithiolates Related to the Active Site of [NiFe]-Hydrogenases. *Organometallics* **2018,** *37* (6), 1050-1061.

43. Li, X.; Sun, H.; Yu, F.; Flörke, U.; Klein, H.-F., C−F Bond Cleavage and Unexpected C−CN Activation by Cobalt Compounds Supported with Phosphine Ligands. *Organometallics* **2006,** *25* (19), 4695-4697.

44. Zheng, T.; Sun, H.; Ding, J.; Zhang, Y.; Li, X., Effect of anchoring group and valent of cobalt center on the competitive cleavage of C–F or C–H bond activation. *J. Organomet. Chem.* **2010,** *695* (15), 1873-1877.

45. Lian, Z.; Xu, X.; Sun, H.; Chen, Y.; Zheng, T.; Li, X., Imine-assisted C–F bond activation using low-valent cobalt compounds supported by trimethylphosphine ligands and formation of novel organic fluorides. *Dalton Trans.* **2010,** *39* (40), 9523-9529.

46. Leclerc, M. C.; Bayne, J. M.; Lee, G. M.; Gorelsky, S. I.; Vasiliu, M.; Korobkov, I.; Harrison, D. J.; Dixon, D. A.; Baker, R. T., Perfluoroalkyl Cobalt(III) Fluoride and Bis(perfluoroalkyl) Complexes: Catalytic Fluorination and Selective Difluorocarbene Formation. *J. Am. Chem. Soc* **2015,** *137* (51), 16064-16073.

47. Lei, H.; Fettinger, J. C.; Power, P. P., Reduction of Terphenyl Co(II) Halide Derivatives in the Presence of Arenes: Insertion of Co(I) into a C–F Bond. *Inorg. Chem.* **2012,** *51* (3), 1821-1826.

48. Przyojski, J. A.; Arman, H. D.; Tonzetich, Z. J., NHC Complexes of Cobalt(II) Relevant to Catalytic C–C Coupling Reactions. *Organometallics* **2013,** *32* (3), 723-732.

49. Smart, K. A.; Vanbergen, A.; Lednik, J.; Tang, C. Y.; Mansaray, H. B.; Siewert, I.; Aldridge, S., Bulky N-heterocyclic carbene and pyridine donor adducts of Co(II) bromide:

Influence on reactivity of stoichiometry, sterics and donor capability. *J. Organomet. Chem.* **2013,** *741-742*, 33-39.

50. Hashimoto, T.; Urban, S.; Hoshino, R.; Ohki, Y.; Tatsumi, K.; Glorius, F., Synthesis of Bis(N-heterocyclic carbene) Complexes of Iron(II) and Their Application in Hydrosilylation and Transfer Hydrogenation. *Organometallics* **2012,** *31* (12), 4474-4479.

51. Malvolti, F.; Trujillo, A.; Cador, O.; Gendron, F.; Costuas, K.; Halet, J.-F.; Bondon, A.; Toupet, L.; Molard, Y.; Cordier, S.; Paul, F., New thiocyanato and azido adducts of the redox-active Fe(η5-C5Me5)(η2-dppe) center: Synthesis and study of the Fe(II) and Fe(III) complexes. *Inorg. Chim. Acta* **2011,** *374* (1), 288-301.

52. Vogel, C.; Heinemann, F. W.; Sutter, J.; Anthon, C.; Meyer, K., An Iron Nitride Complex. *Angew. Chem. Int. Ed.* **2008,** *47* (14), 2681-2684.

53. Scepaniak, J. J.; Young, J. A.; Bontchev, R. P.; Smith, J. M., Formation of Ammonia from an Iron Nitrido Complex. *Angew. Chem. Int. Ed.* **2009,** *48* (17), 3158-3160.

54. Käß, M.; Hohenberger, J.; Adelhardt, M.; Zolnhofer, E. M.; Mossin, S.; Heinemann, F. W.; Sutter, J.; Meyer, K., Synthesis and Characterization of Divalent Manganese, Iron, and Cobalt Complexes in Tripodal Phenolate/N-Heterocyclic Carbene Ligand Environments. *Inorg. Chem.* **2014,** *53* (5), 2460-2470.

55. Keilwerth, M.; Grunwald, L.; Mao, W.; Heinemann, F. W.; Sutter, J.; Bill, E.; Meyer, K., Ligand Tailoring Toward an Air-Stable Iron(V) Nitrido Complex. *J. Am. Chem. Soc* **2021,** *143* (3), 1458-1465.

56. Rungthanaphatsophon, P.; Rath, N. P.; Neely, J. M., Iron(ii) complexes supported by pyrazolyl-substituted cyclopentadienyl ligands: synthesis and reactivity. *Dalton Trans.* **2022,** *51* (11), 4252-4256.

57. Scepaniak, J. J.; Fulton, M. D.; Bontchev, R. P.; Duesler, E. N.; Kirk, M. L.; Smith, J. M., Structural and Spectroscopic Characterization of an Electrophilic Iron Nitrido Complex. *J. Am. Chem. Soc* **2008,** *130* (32), 10515-10517.

58. Maity, A. K.; Murillo, J.; Metta-Magaña, A. J.; Pinter, B.; Fortier, S., A Terminal Iron(IV) Nitride Supported by a Super Bulky Guanidinate Ligand and Examination of Its Electronic Structure and Reactivity. *J. Am. Chem. Soc* **2017,** *139* (44), 15691-15700.

59. Fillman, K. L.; Przyojski, J. A.; Al-Afyouni, M. H.; Tonzetich, Z. J.; Neidig, M. L., A combined magnetic circular dichroism and density functional theory approach for the elucidation of electronic structure and bonding in three- and four-coordinate iron(ii)–N-heterocyclic carbene complexes. *Chem. Sci.* **2015,** *6* (2), 1178-1188.

60. Saber, M. R.; Przyojski, J. A.; Tonzetich, Z. J.; Dunbar, K. R., Slow magnetic relaxation in cobalt N-heterocyclic carbene complexes. *Dalton Trans.* **2020,** *49* (33), 11577-11582.

61. Yambulatov, D. S.; Nikolaevskii, S. A.; Shmelev, M. A.; Babeshkin, K. A.; Korchagin, D. V.; Efimov, N. N.; Goloveshkin, A. S.; Petrov, P. A.; Kiskin, M. A.; Sokolov, M. N.; Eremenko, I. L., Heterometallic Coii-Lii carboxylate complexes with N-heterocyclic carbene, triphenylphosphine and pyridine: a comparative study of magnetic properties. *Mendeleev Commun.* **2021,** *31* (5), 624-627.

62. Kumar Sahu, P.; Kharel, R.; Shome, S.; Goswami, S.; Konar, S., Understanding the unceasing evolution of Co(II) based single-ion magnets. *Coord. Chem. Rev.* **2023,** *475*, 214871.

63. Perdew, J. P.; Burke, K.; Ernzerhof, M., Generalized Gradient Approximation Made Simple. *Phys. Rev. Lett.* **1996,** *77* (18), 3865-3868.

64. Handy, N. C.; Cohen, A. J., Left-right correlation energy. *Mol. Phys.* **2001,** *99* (5), 403-412.

65. Grimme, S.; Antony, J.; Ehrlich, S.; Krieg, H., A consistent and accurate ab initio parametrization of density functional dispersion correction (DFT-D) for the 94 elements H-Pu. *J. Chem. Phys* **2010,** *132* (15), 154104.

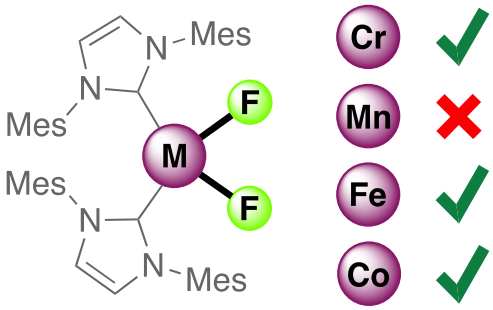

Four-coordinate mononuclear bis-fluoride bis-NHC complexes of Cr(II), Fe(II), and Co(II) were synthesized from corresponding silylamido complexes and IMes•2HF. The synthetic utility of the Fe fluoride complex was demonstrated, taking advantage of Si−F bond strength. X-ray, magnetic, and DFT studies of the resulting complexes were presented.